Evaluation of friction stir welding on the microstructure and mechanical properties of dissimilar aluminum alloys 5083-O and 6061-T6 for automotive applications

Gunawan Dwi Haryadi[1*], Muhammad Taufik[1], Okpina Rochadian[1],
Wahyu Caesarendra[2], Krzysztof Żak[3]

1. Mechanical Engineering Department, Diponegoro University, Jalan Prof. Sudarto, S.H, Semarang, 50275, Indonesia
2. Department of Mechanical and Mechatronics Engineering, Faculty of Engineering and Science, Curtin University Malaysia, Lot 13149, Block 5 Kuala Baram Land District, CDT 250, 98009 Miri, Sarawak, Malaysia
3. Faculty of Mechanical Engineering, Opole University of Technology, ul. Proszkowska 76, 45-758 Opole, Poland
* Corresponding author's e-mail: gunawan_dh@ft.undip.ac.id

ABSTRACT

The friction stir welding (FSW) process, employed for joining aluminium alloys, particularly the 5xxx and 6xxx series, is widely utilized in various applications, notably within the automotive industry. These alloy series exhibit the properties that render them ideal for manufacturing components, such as frames, chassis, and pistons due to their lightweight, strength, and corrosion resistance. FSW is especially advantageous, as it presents an environmentally friendly alternative for aluminum welding, characterized by its low melting point, which facilitates precise thermal control during the welding process. This investigation focuses on the impact of FSW process parameters on the microstructure and mechanical properties of 5083-O and 6061-T6 aluminum alloys, Optimal welding conditions were determined to be a tool rotational speed of 1400 RPM, a travel speed of 30 mm/s, and a tool tilt angle of 1°. Under these parameters, a tensile strength efficiency of 75% relative to the 5083-O base material was achieved, with a maximum tensile strength recorded at 203.8449 MPa and a hardness range of 70.1–70.5 HV. Microstructural analysis reveals a clean weld surface devoid of significant defects that could compromise weld quality. The material exhibited equiaxed recrystallized grains in the WN zone under optimal parameters. Conversely, the most vulnerable aspect of the welded joint was consistently identified within the heat affected zone (HAZ) of the 6061-T6 side across all parameter configurations. This susceptibility is attributed to grain growth and the dissolution of Mg_2Si precipitates induced by the thermal effects during the FSW process, as corroborated by microphotographic analysis.

Keywords: friction stir welding (FSW), heat affected zone (HAZ), weld nugget (WN), Mg_2Si precipitates, micro photograph, mechanical strength.

INTRODUCTION

Recent technological advancements, particularly within the automotive sector, are significantly enhancing competitiveness in the global market. A pivotal strategy for maintaining this competitiveness involves the adoption of lightweight materials, such as aluminum, aimed at minimizing vehicle weight [1]. This reduction contributes not only to improved energy efficiency but also

enhances overall vehicle performance. Aluminum and its alloys possess superior characteristics relative to other metals, exemplified by their excellent thermal conductivity and suitability for replacing traditional steel, which has been extensively utilized in both the automotive and maritime industries. Various joining methods are implemented in this context, with rivet joints being prevalent. This method necessitates the creation of drilled holes in each plate to accommodate rivets. Conversely,

conventional welding practices that utilize electrodes frequently encounter challenges, such as porosity and cracking during the welding of aluminum, primarily attributable to uncontrolled temperature variations throughout the welding procedure [2]. Aluminum alloys find extensive application across numerous industries, particularly in automotive, aviation, and maritime fields. Within the maritime domain, it has been established by Wahid et al. [3] that the 5xxx and 6xxx series aluminum is commonly employed in ship construction, including such components as hulls, superstructures, and deck panels. These alloys are favoured due to their advantageous strength properties, lightweight nature, and exceptional corrosion resistance. Furthermore, in subsea construction, these aluminium variants are similarly utilized in the fabrication of underwater pipe frames.

The joining of aluminium and its alloys presents challenges due to their classification as heat treatable and non-heat treatable materials, which is fundamentally rooted in their distinct chemical structures and melting points [4]. This disparity complicates conventional welding techniques and riveted joints, often compromising the quality, integrity, and weight of the components being fused A promising alternative for achieving robust connections between metals exhibiting differing properties is friction stir welding (FSW). As reported by Thomas W. Thompson of the welding institute (TWI), UK, in 1991 [5] FSW offers numerous advantages over traditional welding methods, including enhanced corrosion resistance, the elimination of joint pits, and the avoidance of harmful emissions such as dust, fumes, and gases, as well as the omission of additional fillers. The FSW process utilizes a specialized tool comprising a pin and shoulder, which mechanically agitates the two metals at the joint interface. This agitation generates sufficient frictional heat to soften the materials, allowing the rotating tool to mix the softened substrates, thereby facilitating the formation of high-quality welds in a comparatively short duration for dissimilar materials.

FSW is extensively employed for the joining of various alloy metals, including aluminum, magnesium, copper, brass, and steel. This technique is particularly advantageous, as it facilitates the welding of aluminum alloys at temperatures below their melting points, thereby minimizing the prevalence of welding defects [6]. Extensive research has been conducted on the FSW process, specifically for 5083-O and 6061-T6 aluminum alloys, focusing on the influences of parameters such as tool rotational speed, travel speed, and tool tilt angle. According to Sasi et al. [7], a thorough investigation into the characterization of FSW in terms of mechanical properties and microstructural changes revealed that the most compromised area of the weld is located in the heat affected zone (HAZ) of the 6061-T6 side, attributable to grain coarsening. Additionally, the overall joint efficiency was determined to be merely 58%, whereas the nugget zone displayed elevated hardness levels due to dynamic recrystallization resulting from the effective mixing of materials during the welding process.

Research on the same topic has also been conducted by Manohar et al. [8] who discussed the mechanical properties of the welding results between 5083-O and 6061-T6 aluminum. The findings indicate that the friction stir welding (FSW) method is particularly effective for joining these materials. Optimal results were observed with a significant reduction in weld grain size when employing a taper threaded pin tool, specifically at a rotation speed of 1400 rpm and a welding speed of 60 mm/s, yielding high welding efficiency. Then research conducted by Guido Di Bella et al. [9] by examining the effect of rotational speed on the mechanical properties of FSW joints of 5083/6061 aluminum alloys for maritime applications. Their findings revealed that a rotational speed of 1400 rpm results in enhanced mechanical properties, characterized by a more uniform hardness distribution attributed to material mixing and optimal thermal input during tool rotation. However, it was noted that excessively high rotational speeds can lead to the formation of wormholes, ultimately diminishing the mechanical strength of the joint. FSW involves critical considerations of axial force and torque during the welding process, with an emphasis on investigating the interrelations among these parameters to optimize welding outcomes. According to the findings of Kai Wu [10], the FSW process facilitates uniform material mixing; however, it also predisposes the process to void formation at elevated rotational speeds. The optimal welding parameters identified include a tool rotation speed of 2400 rpm, a travel speed of 1200 mm/min, and a plunge depth of 0.25 mm.

Another study related to the welding of 5083-O and 6061-T6 aluminum joints was conducted by Devaiah et al. [11], the influence of a tool tilt of 2.5° and a threaded tool geometry on the

microstructural characteristics of welded joints between 5083-O and 6061-T6 aluminum alloys was explored. The results indicated that the optimal tool tilt and threaded configuration yielded superior mechanical and metallurgical properties in comparison to lower tilt angles and threadless tools. This current study aimed to further elucidate the effects of rotational speed and tool tilt on determining the optimal parameters within the FSW process for joining 5083-O and 6061-T6 aluminum alloys. The parameters under examination encompassed tool rotational speeds of 1100 RPM, 1400 RPM, and 1800 RPM, in conjunction with tool tilt angles of 1° and 3°. The primary objective of this research was to ascertain the most advantageous welding parameters through a comprehensive evaluation of the microstructure and mechanical properties of the joint, particularly focusing on the quality of mixing within the weld nugget zone. The outcomes of this investigation are anticipated to yield meaningful recommendations for welding parameters pertinent to industries such as automotive manufacturing.

MATERIALS AND METHODS

Tool pin design

The tool utilized in the FSW process is constructed from H13 steel, exhibiting a hardness metric of 55 HRC. This material undergoes a vacuum hardening procedure to achieve its desired mechanical properties. The pin profile is characterized as a cylindrical tapered thread; this geometric configuration is strategically selected to facilitate a more uniform flow of the workpiece material. During operation, material is conveyed downward on the advancing side, subsequently flowing upward toward the retreating side within the vicinity of the pin. Figure 1

presents a 3D representation of the welding zone in the FSW process. Figure 1 describes the material distribution in the FSW zone. The observed pattern reveals the vertical and horizontal movement of material, a result of the rotation and applied pressure of the tapered threaded pin. This demonstrates the efficacy of the tool design in facilitating material mixing, which significantly mitigates the potential for defects, such as cracks and voids, particularly within the welded region. Consequently, this flow pattern is instrumental in producing the joints characterized by a more homogeneous microstructure and enhanced mechanical properties. The pin design implemented in the FSW process for 5083-O and 6061-T6 aluminum is depicted in Figure 2.

FSW machine and types

In the FSW process under discussion, a GUT DRO × 623 vertical milling machine was employed. During the execution of the welding procedure, 5083 aluminum was positioned on the advancing side, while 6061 aluminum occupies the retreating side. This specific configuration was strategically chosen due to the enhanced corrosion resistance of 5083-O aluminum, which benefits from increased heat generation through friction, proving to be more effective in this position relative to 6061-T6 aluminum. The placement of 6061-T6 aluminum on the retreating side is advantageous, as it minimizes deformation and optimizes the flow of material. The aluminum plates 5083-O and 6061-T6 were meticulously cut to the dimensions of 100 × 50 × 3 mm respectively. The following (Figure 3) delineates the process of FSW conducted between 5083-O and 6061-T6 aluminum.

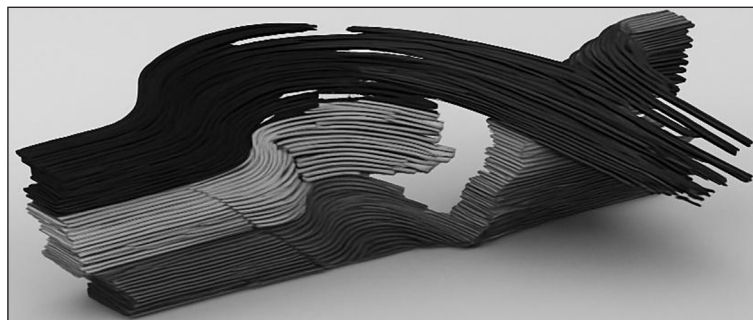The welded plate was subjected to vertical cutting in alignment with the FSW joint to

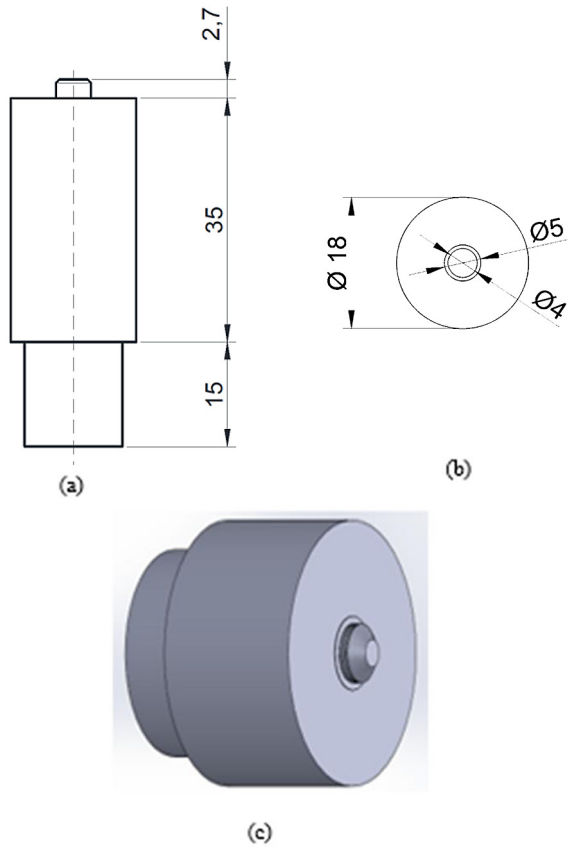**Figure 1.** 3D representation of the FSW area using the tapered thread tool

Figure 2. FSW tapered thread design: (a) tool height, (b) tool diameter, and (c) 3D design

facilitate microstructural and mechanical evaluations of the welding outcomes. The extraction of the test specimen from the welded plate was conducted utilizing TNC-AS cutting metallurgy, ensuring precision while preserving the integrity of the material's microstructure.

Table 1 presents the chemical composition of both tested materials. Additionally, a coolant

was applied to mitigate excessive thermal elevation that could compromise both the mechanical properties and the microstructure of the weld. Subsequent testing of the FSW results was performed using standardized testing apparatus. This included a tensile testing machine, model TC220 series 6604, designed for the assessment of the tensile strength of the weld joint material. Furthermore, a Union Japan metallurgical microscope was employed for the microstructural examination of the weld area, focusing on identifying features such as the heat-affected zone (HAZ), thermo-mechanical affected zone (TMAZ), and the weld nugget (WN). Additionally, a MicroVickers hardness tester (model MVS 1000 AT) was used to determine the microhardness values across various weld zones. The process of testing specimens was carried out on the middle side of FSW joints, such as AA5083-O and AA6061-T6, because in this section there is a more even heat distribution during the welding process. The center side tends to experience a stable welding process and less deformed structure or experience extreme temperature changes that result in the decreasing quality of the welding joint [12].The testing procedure commenced with the preparation of samples measuring 30 × 15 mm, achieved through cutting metallurgy. Thereafter, the Keller reagent was prepared in accordance with established protocols, followed by the mounting of specimens designated for microstructural analysis. Polishing of the relevant zones was executed utilizing a series of sandpapers to achieve a mirror-like finish.

The specimens were then subjected to etching with Keller's solution (composed of 2 ml HF, 3 ml HCl, 20 ml HNO_3, and 175 ml H_2O) before being
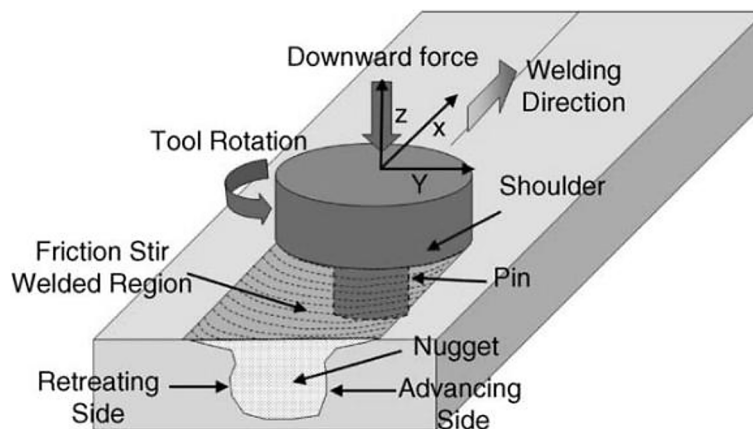

Figure 3. FSW process schematic [12]

Table 1. Chemical composition of aluminum 5083-O and 6061-T6

Alloy	Al	Mg	Si	Mn	Fe	Cu	Zn	UTS, MPa
5083-O	96.78	2.56	0.08	0.019	0.28	0.01	0.02	270
6061-T6	97.45	0.91	0.63	0.13	0.39	0.24	0.03	300

examined under an optical microscope in compliance with ASTM E-407 [13]. Microstructural images were subsequently captured using the optical microscope, with magnifications of 50x, 100x, and 200x. Upon completion of the microstructural evaluation, the etched specimens underwent hardness testing using the Vickers method. A total of 21 hardness measurements were recorded for each specimen, applying a load of 1000 g over a duration of 15 seconds. The Vickers hardness values were measured at 1 mm intervals across the weld zone (Nugget Zone), TMAZ, HAZ, and base metal (BM), adhering to ASTM E 384-22. Finally, tensile test samples were prepared in accordance with ASTM E8 [14] standards, with three specimens tested for each welding parameter. The outcomes were averaged to ascertain the maximum tensile strength, elongation, and yield strength. The results derived from these three specimens per welding variable enabled the identification of the optimal mechanical performance of the welded joints.

Maximum temperature distribution in welding

FSW induces significant plastic deformation in the vicinity of the rotating tool, accompanied by frictional interactions between the tool and the workpiece. These phenomena result in elevated temperatures within and surrounding the stirring zone. The temperature profile in this region plays a crucial role in shaping the weld microstructure, influencing parameters such as grain size, grain boundary characteristics, the hardening and dissolution of precipitates, and the resultant mechanical properties of the weld. Nonetheless, quantifying the temperature within the stirring zone poses substantial challenges due to the pronounced plastic deformation associated with the rotation and movement of the tool. Consequently, the peak temperature in the stirring zone during FSW is typically inferred through an examination of the weld microstructure. As reported by Mishra et al. [12], the maximum temperature in the stir zone frequently

attains approximately 80–90% of the melting point of the base material, which translates to roughly 400–480 °C for 6061 aluminum, with a marginally lower threshold for 5083. A commonly employed formula for predicting temperature distribution follows a specific methodology, while the equation for determining the melting point of a blend of aluminum alloys is articulated in Equation 1.

$$T_{MIXTURE} = \frac{(\omega_1 \times T_1) + (\omega_2 \times T_2)}{\omega_1 + \omega_2} \qquad (1)$$

The average maximum temperature of the aluminum plate is measured as a function of the pseudo heat index ($w = v^2/n$). The primary variables in this equation (Equation 2) consist of the tool's rotational speed (ω), the speed of travel (v), and a constant (K) that varies based on the material type and welding parameters. This correlation indicates that the maximum temperature (T) in relation to the material's melting point (Tm) rises with the square of the rotational speed (ω^2) and declines as the travel speed (v) increases.

$$\frac{T}{T_m} = K \left(\frac{(\omega^2)}{(V \times 10^4)} \right)^\alpha \qquad (2)$$

FSW parameters

The Gut Milling Universal X6332Z machine is utilized in FSW to join two metal pieces intended for welding. This method employs a JIG as a holding chamfer to maintain the stability and immobility of the material being welded, which consistently yields high-quality joints. Key factors in the welding process include tool rotational speed, travel speed, tool tilt angle, and plunge depth at the joint. The rotational speed of the tool generates heat through friction, whereas the welding speed regulates the melting of the material along the welding trajectory. The tilt angle of the tool and the compression force contribute to the stability and uniformity of the weld nugget. These parameters are optimized to ensure that the joint experiences minimal failures during the welding procedure. The subsequent variables will be applied in the FSW process as follows (Table 2).

Table 2. FSW parameters

No.	Specimen	TRS (RPM)	TS (mm/min)	Tool tilt
1.	FSW 1	1100	30	1°
2.	FSW 2	1100	30	3°
3.	FSW 3	1400	30	1°
4.	FSW 4	1400	30	3°
5.	FSW 5	1800	30	1°
6.	FSW 6	1800	30	3°

RESULTS AND DISCUSSION

FSW results between aluminum 5083-O and 6061-T6

The results of FSW of aluminum joints, AA5083 and AA6061, reveal several important features that can influence the mechanical properties and microstructure of the joined material. As a solid-state welding technique, FSW creates a joint without melting the materials. The welding zone is established through frictional heating and plastic deformation during the welding process. Typically, the microstructure in the weld zone experiences dynamic recrystallization, leading to uniform fine grains, which enhances the mechanical strength compared to the pre-weld base material. This research aimed to investigate the welding outcomes of aluminum plates AA5083 and AA6061 with butt joints, by varying the rotational speed and tilt angle of the FSW tool. The findings of this study are presented based on how the chosen parameters affect the results.

Surface appearances of joints and macroscopic metallography

Visual testing of welded joints results on AA5083-O and AA6061-T6 aluminum were made with variations in rotational speed and tool tilt, namely 1100 rpm, 1400 rpm, and 1800 rpm with angles of 1° and 3°. Observations focused on surface smoothness, joint line stability, and defect detection such as cracks, flash, or rough grooves. Surface smoothness reflects the stability of the FSW process; a smooth surface indicates optimal tool interaction without excessive deformation, while a stable joint line indicates suitable rotation parameters and tilt angle to ensure joint continuity. Rotational parameters affect the welding temperature of the tool rotational speed of 1100 rpm produces a maximum temperature of 370 °C, then 1400 rpm produces a maximum temperature of 460 °C, and 100 rpm creates temperatures of up to 520 °C. These temperatures affect the plasticity of the material; high rotations such as 1800 rpm increase plasticity but can potentially cause flash, while low rotations such as 1100 rpm can result in cracks or rough surfaces due to lack of thermal energy. In addition, the tilt angle of the tool affects the distribution of heat and pressure which has a direct impact on the homogeneity of the weld zone structure and the overall quality of the joint. the following is a picture of the welding results between aluminum 5083 and 6061 are as follows. The welding results between AA5083-O and AA6061-T6 aluminum are presented in Figure 4.

The figure above shows macro photographs and frontal views of the welding outcomes from FSW on AA5083-O and AA6061-T6 aluminum, utilizing various welding parameters. Each picture shows the differences in joint quality resulting from changes in tool rotation speed and tilt angle. FSW joints are categorized into BM, HAZ, TMAZ, and WN. Observations of the macro morphology of the samples from parameter 3 indicate that the most favorable results are marked by consistent weld zones, smooth surfaces, and the complete absence of defects like cracks, flash, and rough grooves. The regular joint structure demonstrates that the right combination of rotational speed and tool tilt angle can achieve optimal heat and pressure distribution, leading to a perfect fusion of 5083 and 6061 aluminum materials. The processes of dynamic plastic deformation and recrystallization are optimal, leading to a refined microstructure that enhances the mechanical properties of the joint. Conversely, parameter images 2 and 6 display imperfections in the joint, such as inconsistencies in the joint line, excessive material deformation, or significant flash. These imperfections arise from sub-optimal parameters like excessively high or low rotational speeds and less-than-ideal tilt angles. Elevated rotational speeds can lead to over-plasticization of the material and an excess of flash,
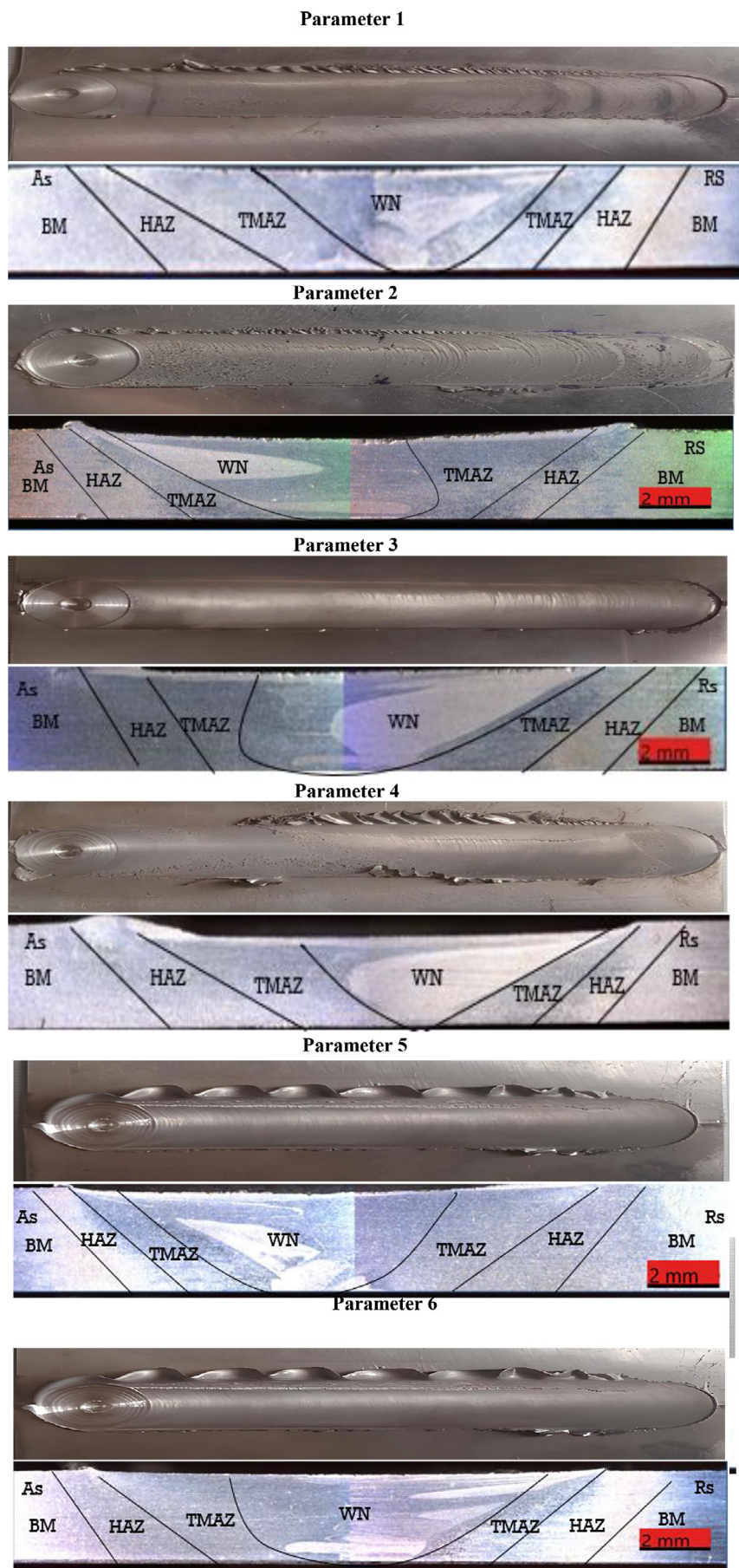
Parameter 1

Parameter 2

Parameter 3

Parameter 4

Parameter 5

Parameter 6

Figure 4. View of the joint between 5083-O and 6061-T6 aluminum alloys

while decreased rotational speeds may result in an uneven material blend, cracks, or rough surfaces. The parameters illustrated in Figure 4 achieve an optimal equilibrium between heat and plastic deformation, yielding a stable weld zone with exceptional joint quality. With these parameters, the joint shows no significant defects, suggesting that the combination of rotational parameters and tilt angle used is well-suited for AA5083 and AA6061 aluminum materials.

Effect of temperature increase on micro yield

The temperature obtained when increasing the rotational speed in the FSW process gives an idea of the effect on the yield microstructure of aluminum 5083-O and 6061-T6, especially on the weld nugget. A rotational speed of 1100 RPM with a 1° tool angle results in a temperature of 379.2°, which leads to enlarged grain crystals in the HAZ of aluminum due to uneven heat distribution and plastic deformation. According to Elangovan et al. [15], as the angle becomes more concave at 3°, the temperature reaches 384.6°, and promotes more significant grain enlargement. This demonstrates that even a minor increase in temperature can heighten sensitivity to heat, which negatively impacts distribution and accelerates grain growth. On the basis of the experimental data collected using a QREM-45 thermometer gun, the welding temperature at the weld endpoint was measured as shown in Figure 5.

Comparison of observations on the HAZ zone of 606

The micro test figures above explain that the FSW process between 5083-O and 6061-T6 aluminum exhibits distinct characteristics for each parameter in Figures 6(a) and (b). Grain boundaries are prominently visible in AA 6061-T6 due to the heating effects, resulting in grains that are
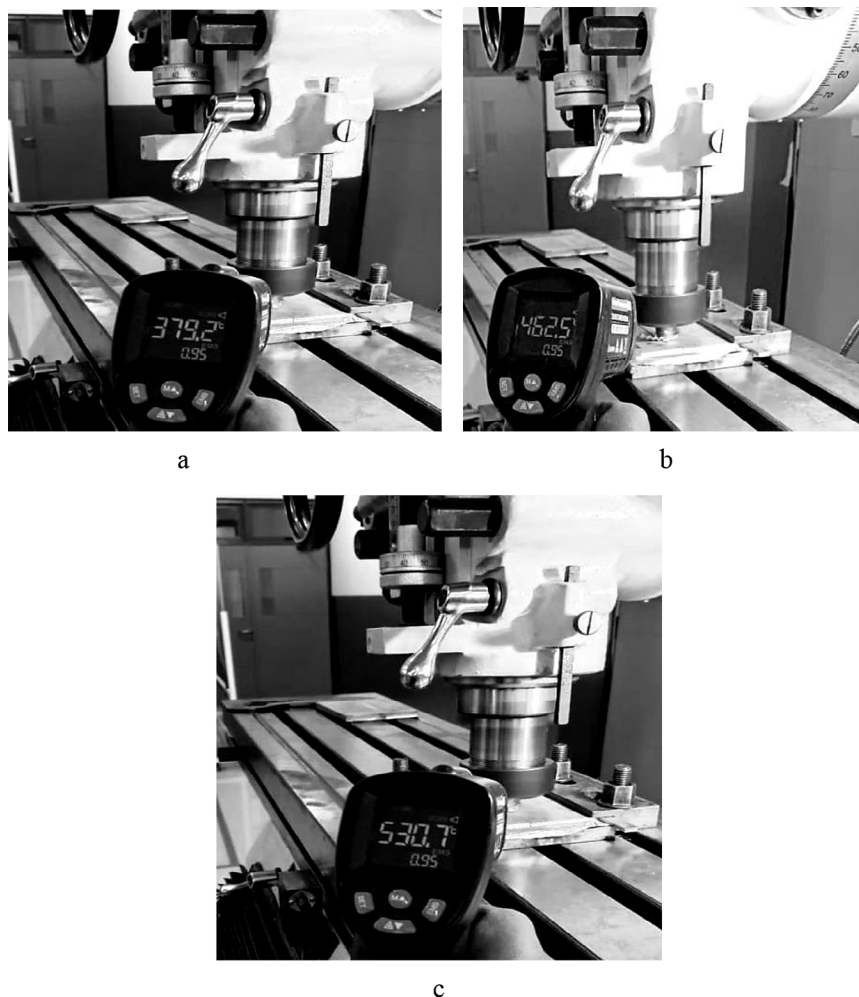

a

b

c

Figure 5. Maximum temperature measurement documentation using thermometer gun QREM-45: (a) Parameter 2, (b) Parameter 3, (c) Parameter 4
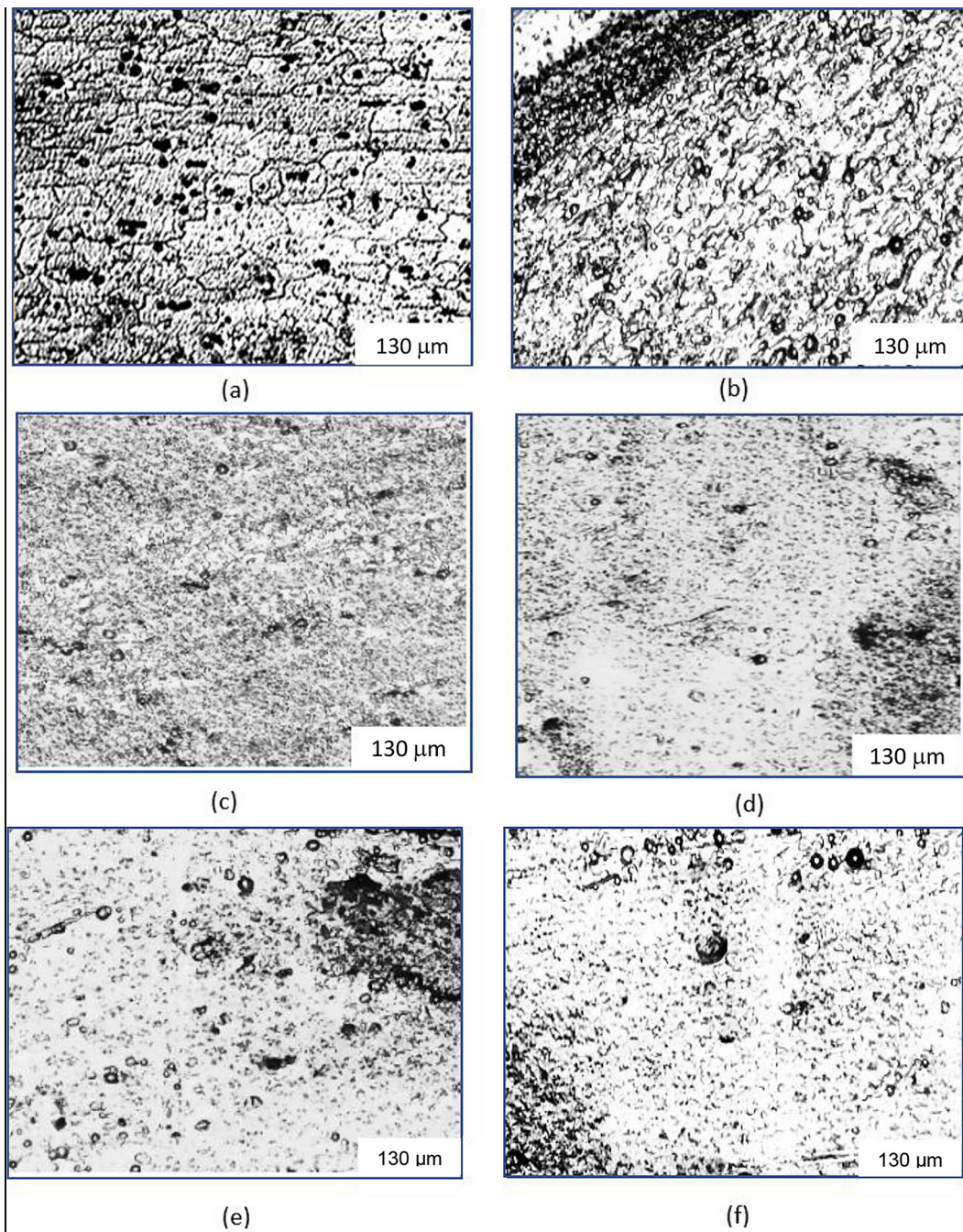
Figure 6. Comparison of HAZ zone of 6061-T6 FSW: (a) Parameter 1, (b) Parameter 2, (c) Parameter 3, (d) Parameter 4, (e) Parameter 5, (f) Parameter 6

exposed but not directly deformed. In Figures 6(c), (d), (e), and (f), it appears that in this zone the amount of Mg_2Si precipitant in the HAZ is drastically reduced, this is due to the increase in grain size making one of the main causes of reduced Mg_2Si precipitant strengthening so that the tensile value and hardness value decrease in this zone. This statement is in accordance with the research conducted by Osorio Dias et al. [16] which states that the 6061-T6 HAZ zone will experience softening due to aging treatment from the stirring

process that generates heat. The maximum temperature that occurs and the recrystallization process cause the dissolution of precipitates so that it can reduce the hardness value of the connection.

Comparison of observations in the Nugent weld zone

In welding dissimilar materials between aluminum 5083-O and 6061-T6, the process parameters have a great impact on the degree of material
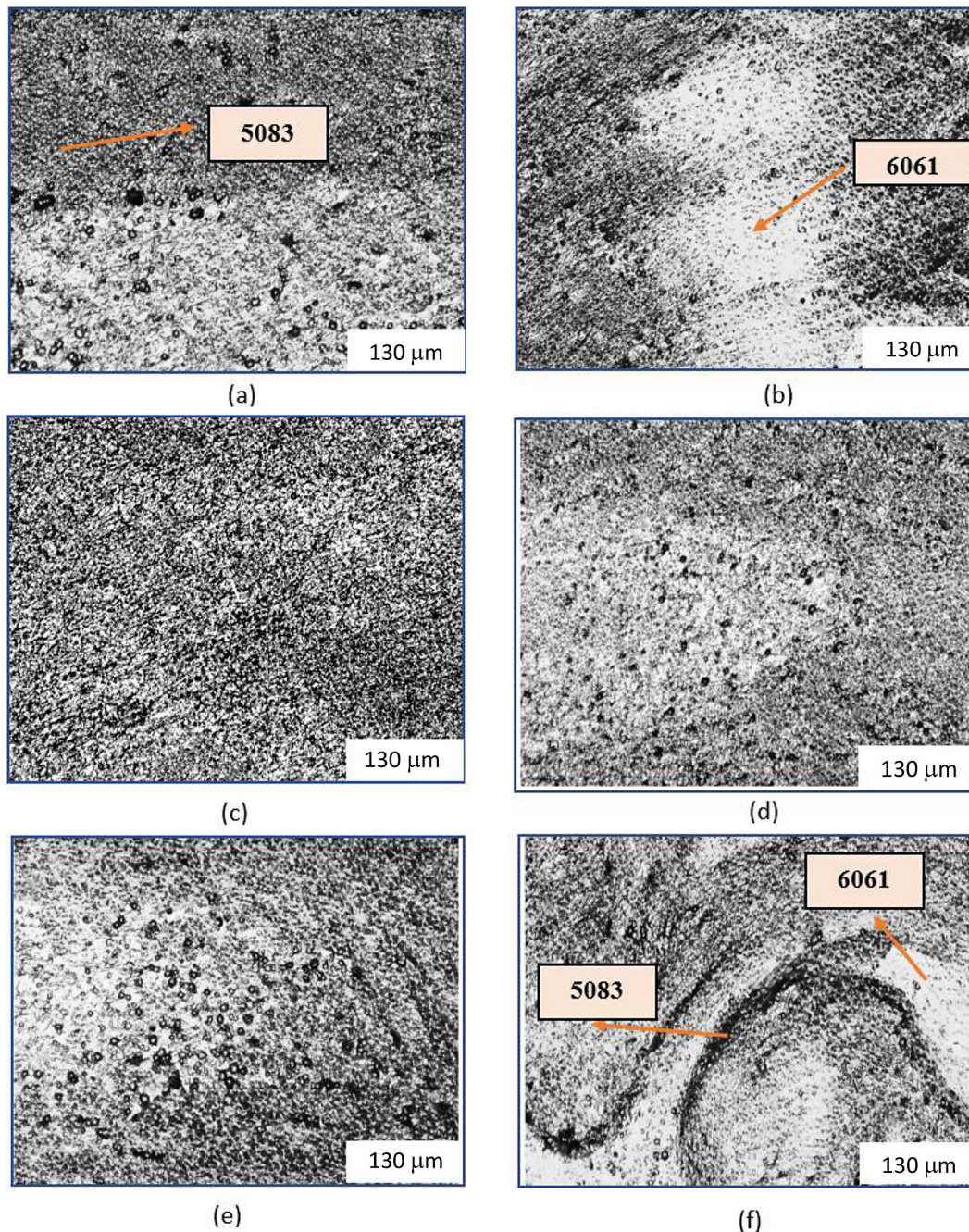
Figure 7. Comparison of WN zones of 5083-O and 6061-T6 FSW aluminum: (a) Parameter 1, (b) Parameter 2, (c) Parameter 3, (d) Parameter 4, (e) Parameter 5, (f) Parameter 6

mixing. In Figure 7(a), the stir zone shows suboptimal mixing, with distinct grain boundaries between aluminum 5083-O and 6061-T6 still apparent. This suggests that the heat energy produced is not sufficient to trigger substantial dynamic recrystallization, causing the resulting plastic deformation to inadequately promote material homogenization. It implies that lower rotational speeds in friction stir welding (FSW) can lead to uneven localized heating, which hampers material diffusion within the stir zone. In Figure 7(b), an excessively steep tool tilt causes asymmetric material flow, while a high tool travel speed (30 mm/s) restricts the interaction between the tool and the materials. The combination of a high travel speed and an excessively steep tool angle may obstruct lateral heat transfer, resulting in uneven material mixing [17].

In Figure 7(c), the grain structure exhibits increased uniformity, suggesting that adequate thermal energy has been generated to initiate dynamic recrystallization. This phenomenon results in a defect-free stirring zone, as confirmed by research

indicating that high rotational speeds enhance material homogenization during FSW, particularly among various aluminum alloys. Conversely, in Figure 7(d), despite the presence of fine grains, the material distribution remains inconsistent, forming a pronounced mountain pattern. This observation illustrates that differences in the thermoplastic properties of the materials can lead to the predominance of one material within the flow of the stirring zone. Specifically, the more ductile aluminum alloy 5083-O tends to assert dominance, while the less ductile aluminum 606-T6 displays a relative lag in the flow dynamics.

In Figure 7(e), the stir zone structure shows the dominance of aluminum 5083-O in some areas, although the grain structure tends to be uniform. This is due to the brief interaction between the tool and the material due to the high travel speed. Research by Xiao et al. [18] noted that high travel speeds in FSW can result in an imbalance between heat input and mechanical deformation, which limits effective material mixing. Then in Figure 7(f) the stirred zone exhibits a more homogenous grain structure characterized by distinct vortex formations. Nonetheless, the demarcation between the two aluminum alloys remains evident, underscoring the differing thermoplastic properties of aluminum 5083 and 6061 as a significant impediment to complete material integration. Furthermore, it has been noted that vortex patterns frequently emerge in the stir zone during FSW, influenced by the interplay of material flow variations derived from differences in material characteristics and process parameters.

Vickers microhardness test results

The distribution of measurement points is used to determine the hardness level of each zone such as BM AS, HAZ AS, TMAZ AS, WN, TMAZ RS, HAZ RS, and BM RS of each group of experimental samples. There are 21 measurement points in each row, with a distance of 0.5 mm between measurement points in the WN zone and 1 mm in other zones. The horizontal coordinate of the central point is established as 0, with the negative direction indicating the AS side and the positive direction on the RS side. The test points are positioned 1.5 mm above and below the center. The hardness is generally highest in the BM, while the hardness observed in the NZ, HAZ, and TMAZ shows a fluctuating trend. Higher temperatures can produce equiaxed grains with small size variations in the stir zone [19]. The results of FSW Evaluation of Friction Stir Welding on the Microstructure and Mechanical Properties of Dissimilar hardness testing, conducted using MicroVickers hardness measurement, are graphically represented to illustrate the correlation between the penetration distance of each indenter relative to the weld center and the measured Vickers hardness number (HV). The graphical representation of the hardness test results is depicted in the subsequent figure (Figure 8). The figure presented elucidates the results of microhardness testing conducted on friction stir welding (FSW) joints between heat treatable aluminum 6061-T6 and non-heat treatable aluminum 5083-O, as stipulated by the parameters specified. It can be seen in the figure that the TMAZ and
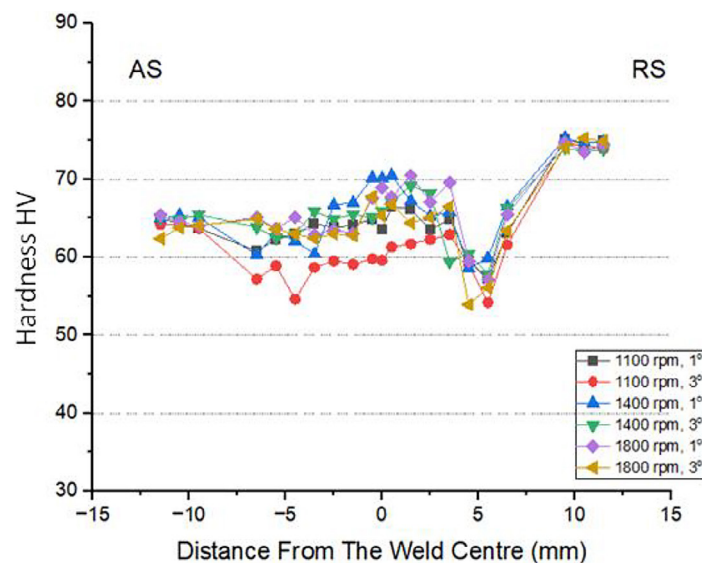

Figure 8. MicroVickers hardness measurement

HAZ zones on the AS (5083-0) side of the test have almost the same hardness value and have a larger grain size than the weld nugget zone, and in this zone there is also an increase in hardness, due to the presence of Mg_2Si precipitants. It can also be seen that the highest hardness value is found in BM 6061-T6, this occurs because there are many Mg_2Si precipitants in BM in the RS section. Figure 8 also shows that the HAZ on the RS side exhibits a significant decrease in hardness, caused by the dissolution of the primary Mg_2Si reinforcement precipitates in the 6061-T6 aluminum base metal due to the heat generated during the FSW process.

The process of dissolving the Mg_2Si precipitates resulted in a decrease in hardness and strength in the HAZ zone of SISI 6061, causing this zone to become the weakest point of the connection welding process. The lowest hardness value occurs in the HAZ zone of 6061-T6 which is caused by the over-aging process that occurs due to heat input during the welding process which causes dissolution of Mg_2Si precipitates and greater grain growth in this zone [19]. The thermal cycling and plastic deformation of the TMAZ zone on the AA6061 side resulted in the dissolution of the Mg_2Si precipitant, thus also affecting the decrease in the strength value of the TMAZ zone on the 6061-T6 side. Figure 8 also proves that the hardness value in the weld nugget zone has a higher value compared to BM 5083-O. This is due to the perfect mixing process in this zone.

Tensile test results

Tensile testing was conducted on the results of FSW of aluminum alloys 5083-O and 6061-T6, adhering to the ASTM E8 standards for specimen preparation, calculation, and modeling. The testing is carried out with a rotation variation of 1100 rpm, 1400 rpm, and 1800 rpm with a tilt angle or tool tilt 1° and 3°. From the data table (Table 3) below, the average value of the maximum tensile strength can be seen from the graph as a comparison to see the highest and lowest values of the welding process.

The analysis presented in Table 3 and Figure 9 demonstrates the tensile properties of FSW joints formed between aluminum alloys 5083-O and 6061-T6. The study provides critical values such as ultimate tensile strength (UTS), yield strength, elongation, and efficiency percentages that are essential for evaluating joint quality and determining optimal welding parameters relevant to specific applications.

According to the test data, the base material (BM) 6061-T6 exhibits a UTS of 300.01 MPa and an elongation of 21.6%, while BM 5083 shows a UTS of 270.5152 MPa with 13.8% elongation. These parameters serve as a reference for assessing welding outcomes. Notably, the results indicate that the highest UTS value, recorded at Parameter 3 (1400 RPM, tool tilt of 1°), is 203.8449 MPa, achieving an efficiency of 75%. This finding suggests that the joint produced under Parameter 3 possesses the strength characteristics that are comparable to those of the base material BM 5083-O, thereby rendering it suitable for the applications necessitating high tensile strength.

Furthermore, this parameter achieves an optimal equilibrium between tensile strength and ductility. The application of a rotational speed of 1400 RPM generates a favorable temperature conducive to microstructural recrystallization, avoiding overheating and preserving mechanical integrity. A welding speed of 30 mm/s facilitates uniform heat distribution, while a tool angle of 1° and a penetration depth of 0.2 mm enhance bond quality, mitigating the risk of defects such as voids or porosity. In parameter 6,

Table 3. Tensile strength test properties

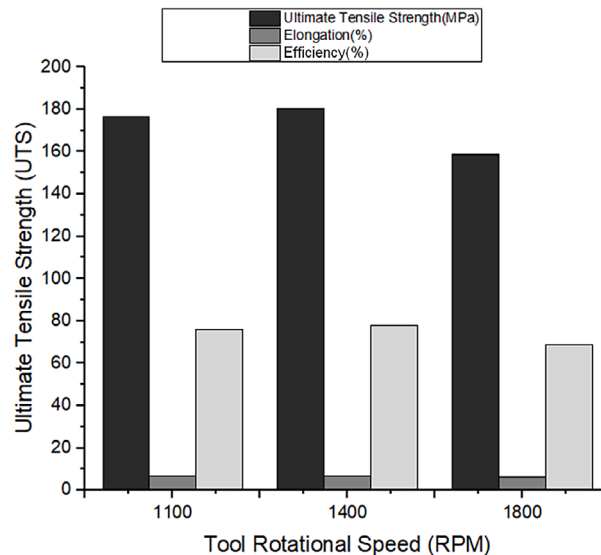| Parameter	UTS, MPa	Yield strength, MPa	Extension, %	Efficiency, %
BM 6061-T6	300.01	275.59	21.6	-
BM 5083-O	270.51	219.41	13.8	-
1	171.04	115.41	12.1	63
2	165.05	101.84	12.06	61
3	203.84	143.15	13.67	75
4	195.13	126.08	13.07	72
5	190.43	115.44	13.06	70
6	186.37	112.89	16.96	69

Figure 9. Tensile strength test results with different parameters

characterized by a rotational speed of 1800 rpm and a tool tilt angle of 3°, the sample exhibits the highest elongation of 16.967%. This value surpasses that of BM 5083, indicating enhanced ductility and a greater capacity to endure deformation without fracturing. Although the UTS is measured at 186.3769 MPa, the significant elongation observed can be attributed to microstructural alterations within the weld zone induced by the FSW process. The grain recrystallization occurring during the welding process contributes to a refined microstructure, leading to a reduction in tensile strength while simultaneously enhancing ductility. The presence of smaller, more uniform grain sizes in the weld zone facilitates more consistent strain distribution, permitting the material to resist greater deformation prior to cracking. Additional factors influencing this behavior include the welding parameters, such as temperature and tool speed, which can foster microstructural conditions that prioritize elongation over tensile strength. Consequently, the material in specimen 6 is particularly suitable for applications demanding significant deformation capabilities while maintaining low levels of tensile stress. This observation aligns with the findings of Kumar et al. [20], which propose that increased elongation is typically associated with process parameters that yield high heat input, thereby promoting grain refinement within the mixing zone. This synergy renders parameter 6 ideal for scenarios requiring flexibility and tolerance to deformation. In comparison, Parameter 2 exhibited the least favorable mechanical

properties, presenting a UTS of merely 165.0542 MPa, a yield strength of 101.847 MPa, and an efficiency of 61%. These values suggest that the joint produced under these conditions is suboptimal and may demonstrate a higher susceptibility to failure relative to other joints. The diminished performance associated with Parameter 2 (1100 rpm, 3°) can be attributed to the inadequate tool rotation speed and the excessively concave tilt angle of the tool. This configuration results in a grain structure that is misaligned in multiple directions due to the pronounced concavity of the trough angle. Consequently, the frictional interaction between both sides of the workpiece is compromised, leading to grain coarsening, which adversely impacts the material's mechanical properties. This observation aligns with the research conducted by [21], which investigated the influence of rotational speed variations on microstructural outcomes. It was noted that at a rotational speed of 1100 rpm, the weld beads exhibit roughness, and the bond strength of the weld is diminished, corroborating the notion of suboptimal rotational speed. Moreover, the disparity in mechanical properties between aluminum alloys 5083 and 6061 contributes to differences in plasticity and may negatively affect ductility, particularly when the weld zone is dominated by the harder alloys, as also demonstrated in studies [9, 22]. The most effective tensile test graph from the current study is presented below (Figure 10):

On the basis of the stress-strain graph presented for FSW of 5083-O and 6061-T6 aluminum

utilizing various parameter combinations, it is evident that Parameter 3 yields the highest UTS value of 203.8449 MPa, accompanied by a joint efficiency of up to 75% and a ductility of 13.67%. The average results depicted in the figure indicate that all evaluated welding parameters result in UTS values lower than those of the base materials. Notably, Parameter 6 demonstrates the greatest elongation value in the welded joint, achieving 16.97%. This enhancement in elongation reflects a superior ductility of the material, contributing to increased resistance against cracking and impact. The scientific novelty of this research lies in the demonstrated ability to optimize mechanical properties through the strategic combination of welding parameters and the adherence to precise procedures. This study reveals an improvement in joint efficiency relative to previous investigations, facilitated by the application of innovative parameter combinations within the FSW process.

The findings not only enhance the strength and ductility of the welded joints but also introduce an efficient and applicable approach for the FSW of 5083-O and 6061-T6 aluminum alloy.

An analysis of flaw locations in the specimens indicates that the imperfections present in Parameter 3 are as shown in Figure 11. The tensile test specimen shown in the Figure 11 above represents the result of FSW between aluminum 5083-O and 6061-T6 using parameter 3. The failure zone is identified in the welded specimen, as indicated in Figure 11(a). The defect region reveals that failure during the tensile testing occurred within the HAZ of the 6061-T6 portion, corroborating the initial observations from microstructure examination and hardness assessments. In this specific zone, the dissolution of Mg_2Si precipitates transpires due to the elevated temperatures generated during the FSW process, leading to a significant reduction in hardness values. This area,
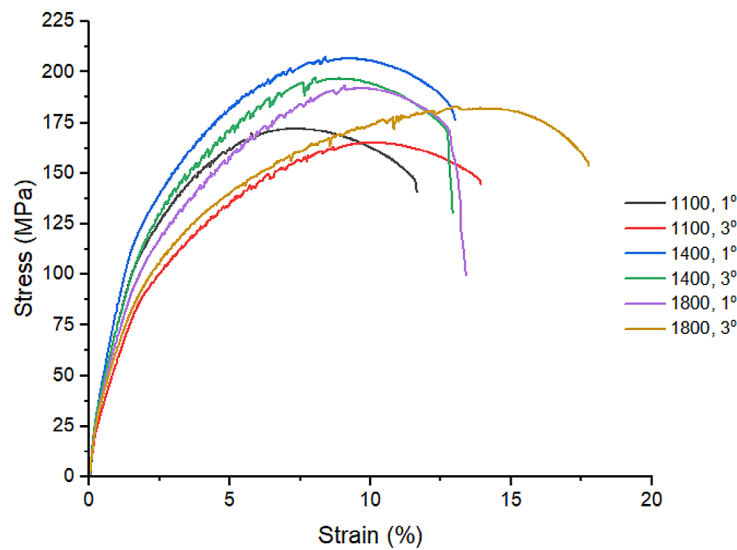

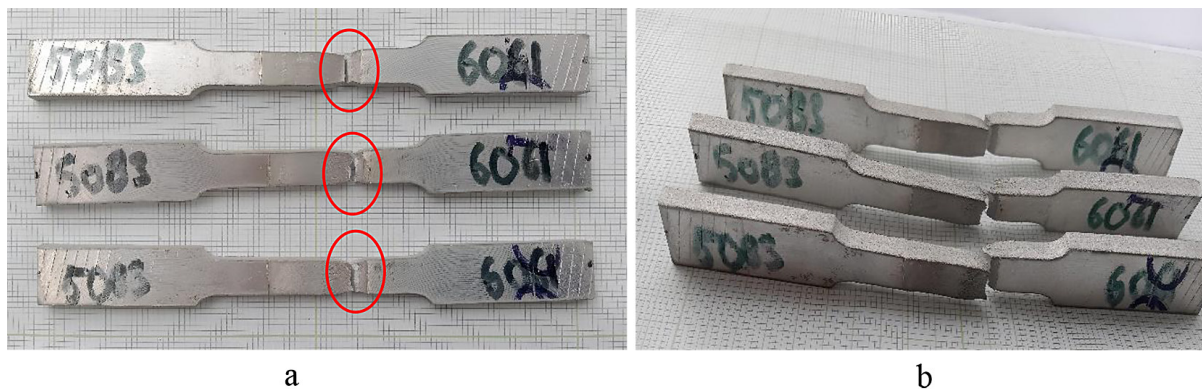**Figure 10.** FSW stress-strain curves

Figure 11. Fracture location of tensile specimens (a) front view, (b) side view

while subjected to heat, remains below the melting point, resulting in altered material properties as a consequence of the frictional forces during welding. As illustrated in Figure 11(b), the side view of the tensile test specimen demonstrates a fracture occurring at a 45-degree angle within the HAZ of the AA 6061-T6 side, identified as the most susceptible zone within the welding joint. This observation aligns with previously analyzed UTS and elongation values, supporting the conclusion that the parameter combination employed is effective in yielding a robust and ductile welded interface between aluminum alloys 5083-O and 6061-T6 [23].

CONCLUSIONS

In this research on friction stir welding studies on straight joints (butt joints) of dissimilar metals, specifically aluminum 5083-O and 6061-T6, it can be concluded that the best mechanical properties are achieved with a tool speed of 1400 rpm, a travel speed of 30 mm/s, and a tilt angle of 1°, resulting in a tensile strength efficiency of 75% compared to the base material 5083. For the type of joint with the lowest tensile strength using welding parameters TRS 1100 rpm, travel speed 30 mm/s, tool tilt 3° with an efficiency of 61%. The following conclusions can be drawn from this research: The analysis of microphotographs indicates that the most vulnerable region of the friction stir weld (FSW) between 5083-O aluminum and 6061-T6 aluminum is in HAZ zone, on the AA6061-T6 side. This vulnerability is attributed to the pronounced growth of grains and grain boundaries, as evidenced through optical microscopy.

The optimal welding parameters are identified as a tool rotation speed of 1400 rpm, a feed rate of 30 mm/s, and a tool tilt angle of 1°. These settings facilitate the formation of a clean and uniform weld surface, devoid of significant defects, such as voids or excessive flash, while ensuring minimal material mixing between the 5083-O and 6061-T6 aluminum alloys. Under these conditions, the weld nugget (WN) zone exhibited the highest hardness values, ranging from 70.1 to 70.5 HV, and displayed a homogeneous grain structure. Additionally, the UTS achieved 203.8449 MPa, corresponding to a joint efficiency of 75%, reflective of a robust connection closely resembling the properties of the 5083-O base material.

The elevated hardness observed in the WN zone under these parameters can be attributed to the equiaxed recrystallization resulting from the uniform mixing facilitated by the pin and tool interaction. This phenomenon is corroborated by microphotographs, which reveal relatively consistent grain sizes, leading to increased hardness in the WN zone. Conversely, the lowest hardness values across all parameters were recorded in the HAZ zone on the 6061-T6 side, primarily due to the dissolution of Mg_2Si precipitates.

Total tool speed, quantified as TRS, exhibits a substantial influence on welding outcomes. An optimal medium rotational speed (1400 RPM) establishes an ideal thermal profile conducive to enhanced material mixing, tensile strength, and hardness. Conversely, a lower rotational speed (1100 RPM) does not provide sufficient heat, whereas an elevated speed (1800 RPM) results in thermal overruns, particularly when working with 6061 aluminum, leading to excessive flash and mechanical degradation. Tool tilt also plays an important role; a 1° angle results in stable pressure and controlled material flow, while a 3° angle results in uncontrolled material flow and material spillage.

Acknowledgment

REFERENCES

1. Zhang W., Xu J. Advanced lightweight materials for Automobiles: A review, Mater. Des. 2022; 221: 110994. https://doi.org/10.1016/j.matdes.2022.110994

2. Verma S., Kumar V. Optimization of friction stir welding parameters of dissimilar aluminium alloys 6061 and 5083 by using response surface methodology, Proc. Inst. Mech. Eng. Part C J. Mech. Eng. Sci. 2021; 235(23): 7009–7020. https://doi.

org/10.1177/09544062211005804

3. Wahid M.A., Siddiquee A.N., Khan Z.A. Aluminum alloys in marine construction: characteristics, application, and problems from a fabrication viewpoint, Mar. Syst. Ocean Technol. 2020; 15(1): 70–80. https://doi.org/10.1007/s40868-019-00069-w

4. Devaiah D., Kishore D.K., Laxminarayana D.P. Effect of material location and tool rotational speed on the mechanical properties of dissimilar friction stir welded Aluminum Alloys (5083-H321to 6061-T6), Bonfring Int. J. Ind. Eng. Manag. Sci. 2016; 6(4): 186–190. https://doi.org/10.9756/bijiems.8311

5. Thomas W.M. Friction stir welding and related process characteristics, INALCO'98, 7 th Int. Conf. Joints Alum. Abington, Cambridge, UK 1998; March: 15–17. Online, Available: https://www.twi-global.com/technical-knowledge/published-papers/friction-stir-welding-and-related-friction-process-characteristics-april-1998#:~:text=In friction joining and forming,friction welding have been reported.

6. Malopheyev S., Vysotskiy I., Kulitskiy V., Mironov S., Kaibyshev R. Optimization of processing-microstructure-properties relationship in friction-stir welded 6061-T6 aluminum alloy, Mater. Sci. Eng: A. 2016; 662: 136–143. https://doi.org/10.1016/j.msea.2016.03.063

7. Rajaseelan S.L., Kumarasamy S. Mechanical properties and microstructural characterization of dissimilar friction stir welded AA5083 and AA6061 aluminium alloys, Mechanika 2020; 26(6): 545–552. https://doi.org/10.5755/j01.mech.26.6.25255

8. Manohar B. Effect of microstructure and mechanical properties of Friction Stir Welded Dissimilar AA5083-AA6061 Aluminium Alloy Joints, Int. J. Res. Eng. Technol. 2016; 5(11): 58–62. https://doi.org/10.15623/ijret.2016.0511011

9. Bella G.Di., Borsellino C., Chairi M., Campanella D., Buffa G. Effect of rotational speed on mechanical properties of AA5083/AA6082 Friction Stir Welded T-Joints for Naval Applications, MDPI-Metals 2024; 14(12):1410. https://doi.org/10.3390/met14121410

10. Jia H., Wu K., Sun Y., Hu F., Chen G. Evaluation of axial force, tool torque and weld quality of friction stir welded dissimilar 6061/5083 aluminum alloys, CIRP J. Manuf. Sci. Technol., 2022; 37: 267–277. https://doi.org/10.1016/j.cirpj.2022.02.003

11. Devaiah D., Kishore K., Laxminarayana P. Optimal FSW process parameters for dissimilar aluminium alloys (AA5083 and AA6061) Using Taguchi Technique, Mater. Today Proc. 2018; 5(2): 4607–4614. https://doi.org/10.1016/j.matpr.2017.12.031

12. Mishra R.S., Ma Z.Y. Friction stir welding and processing, Mater. Sci. Eng. R. Reports 2005; 50(1–2): 1–78. https://doi.org/10.1016/j.mser.2005.07.001

13. ASTM International, Standard Practice for Microetching Metals and Alloys ASTM E-407, 2016; 07 no. Reapproved 2015: 1–22. https://doi.org/10.1520/E0407-07R15E01.2

14. ASTM International, ASTM E8/E8M standard test methods for tension testing of metallic materials 1, Annu. B. ASTM Stand. 4, 2010; no. C: 1–27. https://doi.org/10.1520/E0008

15. Elangovan K., Balasubramanian V. Influences of pin profile and rotational speed of the tool on the formation of friction stir processing zone in AA2219 aluminium alloy, Mater. Sci. Eng.: A 2007; 459(1–2): 7–18. https://doi.org/10.1016/j.msea.2006.12.124

16. Osorio Díaz M.A., Franco Arenas F., Unfried-Silgado J. Effects of process parameters on mechanical properties and microstructure of AA6063-T6 and AA5052-H32 dissimilar Friction Stir Welded joints, Soldag. e Insp. 2024; 29: 1–11. https://doi.org/10.1590/0104-9224/SI29.11

17. Malik V., Kailas S.V., Understanding the effect of tool geometrical aspects on intensity of mixing and void formation in friction stir process, Proc. Inst. Mech. Eng. Part C J. Mech. Eng. Sci. 2021; 235(4): 744–757. https://doi.org/10.1177/0954406220938410

18. Xiao S., Deng Y., Zeng J., Zhang W., Huang L. Effect of heat input on microstructure and mechanical properties of Friction Stir Welded AA2024 and AA7075 Dissimilar Alloys, J. Mater. Eng. Perform. 2021; 30(11): 7989–7997. https://doi.org/10.1007/s11665-021-06000-y

19. Hirata T. et al. Influence of friction stir welding parameters on grain size and formability in 5083 aluminum alloy, Mater. Sci. Eng.: A. 2007; 456(1–2): 344–349. https://doi.org/10.1016/j.msea.2006.12.079

20. Kumar K.K., Kumar A., Nagu K. Mechanical and corrosion behaviour of friction stir welded 5083–6061 aluminium alloy joints: effect of base material position, trans. Indian Inst. Met. 2023; 76(7): 1985–1996. https://doi.org/10.1007/s12666-023-02906-4

21. Ghaffarpour M., Aziz A., Hejazi T.H., Optimization of friction stir welding parameters using multiple response surface methodology, Proc. Inst. Mech. Eng. Part L J. Mater. Des. Appl. 2017; 231(7): 571–583. https://doi.org/10.1177/1464420715602139

22. Baghdadi A.H., Sajuri Z., Keshtgar A., Sharif N.M., Rajabi A. Mechanical property omprovement in dissimilar Friction Stir Welded Al5083/Al6061 Joints: Effects of post-weld heat treatment and abnormal grain growth, MDPI-Materials 2022; 15(1): 288. https://doi.org/10.3390/ma15010288

23. Verma M., Ahmed S., Saha P. Challenges, process requisites/inputs, mechanics and weld performance of dissimilar micro-friction stir welding (dissimilar μFSW): A comprehensive review, J. Manuf. Process. 2021; 68, Part A: 249–276. https://doi.org/10.1016/j.jmapro.2021.05.045